Journal of Cellular Biochemistry 85:101–111 (2002)
DOI 10.1002/jcb.10112

Analysis of the Carboxypeptidase D Cytoplasmic Domain: Implications in Intracellular Trafficking

Elena Kalinina, Oleg Varlamov, and Lloyd D. Fricker*

Department of Molecular Pharmacology, Albert Einstein College of Medicine, Bronx, New York 10461

Abstract Metallocarboxypeptidase D (CPD) is a type 1 transmembrane protein that functions in the processing of proteins that transit the secretory pathway. Previously, CPD was found to be enriched in the *trans* Golgi network (TGN) and to cycle between this compartment and the cell surface. In the present study, the roles of specific regions of the CPD cytosolic tail in intracellular trafficking were investigated in the AtT-20 cell line. When the CPD transmembrane region and cytosolic tail are attached to the C-terminus of albumin, this protein is retained in the TGN and cycles to the cell surface. Deletion analysis indicates that a C-terminal region functions in TGN-retention; removal of 10 amino acids from the C-terminus greatly increases the amount of fusion protein that enters nascent vesicles, which bud from the Golgi, but does not affect the half-life of the fusion protein or the ability of cell surface protein to return to the TGN. Because the 10-residue deletion disrupts a casein kinase 2 (CK2) consensus site, the two Thr in this site (TDT) were mutated to either Ala (ADA) or Glu (EDE). Neither mutation has an increased rate of budding from the TGN, although the ADA mutant has a shorter half-life than either the wild type sequence or the EDE mutant. Adaptor protein-1 and -2 bind to most of the deletion mutants, the EDE point mutant, and the CK2-phosphorylated CPD tail, but not to the wild type tail. Taken together, these results suggest that CPD localization to the TGN requires both static retention involving the C-terminal domain and phosphorylation at a CK2 site, which regulates the binding of adaptor proteins. J. Cell. Biochem. 85: 101–111, 2002.

Key words: peptide processing; furin; AP-1; AP-2

CPD was discovered in a search for carboxypeptidase E-like enzymes in *fat/fat* mice [Song and Fricker, 1995]. These mice lack carboxypeptidase E activity due to a point mutation within the coding region of the gene [Naggert et al., 1995], but are still able to carry out a reduced amount of neuroendocrine peptide processing [Naggert et al., 1995; Fricker et al., 1996; Rovere et al., 1996; Cain et al., 1997; Lacourse et al., 1997; Udupi et al., 1997]. CPD has carboxypeptidase E-like enzyme properties, but differs in several respects. Whereas carboxypeptidase E is a soluble protein at neutral pH that binds peripherally to membranes at pH 5.5 [Fricker et al., 1990; Fricker, 1998a], CPD is a type 1 membrane protein [Kuroki et al., 1995; Song and Fricker, 1996; Tan et al., 1997; Xin et al., 1997; Fricker, 1998b]. The distribution of these two proteins is also different. Carboxypeptidase E is primarily neuroendocrine and is enriched in the regulated secretory vesicles while CPD has a broader tissue distribution and is enriched in the TGN [Song and Fricker, 1996; Xin et al., 1997; Varlamov and Fricker, 1998; Varlamov et al., 1999a]. Both enzymes are specific for C-terminal basic residues (Lys, Arg), but cleave a broad range of substrates containing these C-terminal residues [Fricker, 1998a,b]. Carboxypeptidase E is primarily involved in the processing of neuroendocrine peptides within the late secretory pathway (following the action of prohormone convertases 1 and 2), while CPD functions primarily in the processing of proteins within the TGN and/or immature secretory

Elena Kalinina and Oleg Varlamov contributed equally to this work.

Grant sponsor: NIH; Grant number: DK-55711; Grant sponsor: Research Scientist Development Award (to L.D.F.); Grant number: DA-00194; Grant sponsor: Cancer Center; Grant number: CA13330.

*Correspondence to: Prof. Lloyd D. Fricker, Ph.D., Department of Molecular Pharmacology, Albert Einstein College of Medicine, 1300 Morris Park Avenue, Bronx, NY 10461. E-mail: fricker@aecom.yu.edu

Received 23 August 2001; Accepted 3 December 2001

vesicles (following the action of furin and related TGN endopeptidases).

As previously found with furin and other TGN proteins, CPD cycles to the cell surface and returns to the TGN [Varlamov and Fricker, 1998]. The 58 residue cytosolic tail of CPD is required for the intracellular trafficking of CPD. Removal of all, but a few amino acids of the tail eliminates the retrieval from the cell surface to the TGN [Eng et al., 1999]. Attachment of the transmembrane domain and the 58 residue cytosolic tail of CPD to the C-terminus of albumin leads to the targeting of albumin to the TGN [Varlamov et al., 2001]. The CPD tail on this fusion protein was also found to be phosphorylated in vivo on Thr, and casein kinase 2 (CK2) was found to phosphorylate two Thr within the CPD tail in vitro [Varlamov et al., 2001]. Also, CPD was recently found to bind protein phosphatase 2A, raising the possibility that phosphorylation and dephosphorylation regulate the trafficking of CPD [Varlamov et al., 2001].

The purpose of the present study was to investigate the role of various regions of the CPD tail on different aspects of protein trafficking, with an emphasis on the two Thr residues that can be phosphorylated by CK2. Previously, deletion mapping of duck CPD suggested that an element present in the C-terminal 12 residues was important for retention of CPD in the TGN or in a TGN-recycling loop; removal of this region led to a shorter half-life of the protein and a rapid loss from TGN-like structures when protein synthesis was eliminated with cycloheximide treatment [Eng et al., 1999]. Mutation of the CK2 sites in this region (TDT to ADA) slightly reduced the half-life of duck CPD [Eng et al., 1999]. This previous study used intact duck CPD, including the lumenal domain, and it was not clear if this lumenal domain contributed to the routing of the protein. Furthermore, the effect of substitution of acidic residues within the CK2 sites was not examined. To address these issues, we examined deletion mutants of the CPD tail when attached to the C-terminus of albumin using a variety of techniques to quantitate the intracellular trafficking. In addition, the effect of substitution of the TDT with both ADA and EDE was examined. Finally, the effect of these deletion and point mutants on the binding of candidate interacting proteins was examined. Taken together, the results of these analyses suggest that the binding of adaptor proteins to the CPD tail is largely dependent on the phosphorylation state of the CK2 sites.

MATERIALS AND METHODS

Plasmid Construction, Protein Expression, and Recombinant Protein Production

Human albumin C-terminally fused with the transmembrane and the cytoplasmic domains of duck CPD (Alb-CPD tail) was constructed using the pcDNA3 plasmid containing the coding region of human albumin as described [Varlamov et al., 2001]. Deletion and point mutants of the CPD tail were generated by polymerase chain reaction using the Alb-CPD tail/pcDNA3 plasmid as a template. The reaction products were digested with Xho1/AflII and subcloned into the Xho1/AflII sites of the Alb-CPD tail/pcDNA3 plasmid. The constructs were transfected into AtT-20 cells using the Lipofectin transfection kit (GIBCO-BRL). Stable cell lines were selected using 1 mg/ml Geneticin (G418). Clones expressing Alb-tail construct were identified by Western blot analysis using an antiserum to human serum albumin (Calbiochem). GST-fusion proteins containing the CPD tail were prepared as previously described [Varlamov et al., 2001].

Trafficking Assays

To measure half-life, AtT-20 cells expressing albumin fusion proteins were labeled for 20 min with ^{35}S-Met, chased in unlabeled Met, and analyzed as described for gp180 [Eng et al., 1999], except that albumin fusion proteins were immunoprecipitated using an antiserum to human albumin (Calbiochem).

To measure transport from the TGN to the plasma membrane, At T-20 cells expressing the albumin-CPD tail fusion proteins were metabolically labeled for 20 min with ^{35}S-Met, and then incubated for 90 min at 18.5°C to allow the labeled proteins to accumulate in the TGN. Following the incubation, the cells were washed with cold phosphate buffered saline (PBS), and then incubated at 37°C in PBS containing 1 mg/ml EZ-Link Sulfo-NHS-SS-Biotin (Pierce). The cells were washed, lysed, and subjected to immunoprecipitation using antibodies to human albumin. The immunoprecipitated material was eluted from the protein A beads with 3 M KSCN/0.5% NP-40, diluted 10-fold with 10 mM Tris-HCl pH 8, 0.15 M NaCl, 1 mM EDTA, 0.1% NP-40, and then incubated with strepta-

vidin-agarose (Sigma). The streptavidin-bound albumin represents the cell surface-derived material. Following the incubation, the streptavidin beads were washed with buffer, boiled in SDS-containing gel-loading buffer, and the extracts analyzed on a denaturing polyacrylamide gel.

To measure the rate of endocytosis, AtT-20 cells expressing the albumin-CPD tail proteins were labeled with ^{35}S-Met for 4 h, surface-labeled with EZ-Link Sulfo-NHS-SS-Biotin at 4°C, and then recultured at 37°C. At different time points, the cell surface biotin label was removed by treating cells with the membrane impermeable thiol glutathione (GSH) at 4°C. Control dishes were frozen immediately after biotinylation without GSH treatment to determine the total amount of biotinylated albumin-CPD tail. The biotinylated Alb-CPD tail was immunoabsorbed and isolated on streptavidin agarose as described above.

The in vitro vesicle budding assay was performed as described for gp180 and other proteins [Varlamov et al., 1999b]. The resulting fractions were subjected to immunoprecipitation [Milgram and Mains, 1994] using antibodies to human albumin (Calbiochem).

Immunofluorescence Microscopy and Antibody Uptake Experiments

AtT-20 cells expressing the albumin fusion proteins were analyzed by immunofluorescence as described for CPD [Varlamov and Fricker, 1998] using an antiserum to human albumin (dilution 1:1,000). Antibody uptake experiments were performed as described for gp180 [Eng et al., 1999]. Briefly, AtT-20 cells expressing the albumin fusion proteins were incubated for 40 min at 4°C in Dulbecco's modified Eagle's medium containing a rabbit antibody to human albumin (1:150 dilution), 5 mg/ml nonfat milk, and 20 mM HEPES pH 7.4. Unbound antibody was removed by washing with cold medium and the cells were incubated at 37°C for 30 min to allow for internalization from the cell surface. In some experiments, CY3-labeled transferrin (the gift of Jonathan Backer) was included in the chase. The cells were fixed and stained with fluorescein isothiocyanate-conjugated secondary antibodies to rabbit IgG. For comparison of the internalized Alb-containing protein to a TGN marker, cells were stained with a 1:1,000 dilution of mouse monoclonal antibody to syntaxin-6 (the gift of Dr. Richard Scheller), and then 1:100 dilution of Texas red-labeled anti-mouse IgG, as described [Varlamov et al., 2001].

Binding of Proteins to the CPD Tail In Vitro

Thirty micrograms of the GST-CPD tail fusion proteins were incubated for 40 min at 37°C with 100 μl bovine brain cytosol in 25 mM HEPES, pH 7.2 containing 25 mM KCl, 2.5 mM $MgCl_2$, 1 mM phenylmethylsulfonyl fluoride and 1 μg/ml leupeptin. The GST proteins were adsorbed to the glutathione-Sepharose 4B beads (Pharmacia Biotech, Sweden) at room temperature, washed five times with binding buffer, and then boiled in SDS-loading buffer and analyzed on a Western blot using monoclonal antibodies to gamma-adaptin, AP-1 (clone 100/3, Sigma, 1:200 dilution) and to alpha-adaptin, AP-2 (clone 100/2, Sigma, 1:100 dilution). Antibodies were detected with the SuperSignal enhanced chemioluminescent system (Pierce).

To study the effect of CK2 phosphorylation on adaptor binding, the GST-CPD tail protein (full-length) was first phosphorylated with CK2 according to the manufacturer's instructions (Sigma), and then incubated with bovine brain cytosol as described above. To minimize dephosphorylation of the CPD tail during this incubation, the buffer contained a mixture of phosphatase inhibitors (10 mM NaF, 10 mM Na vanadate, and a 1:500 dilution of Sigma phosphatase inhibitor cocktail).

RESULTS

To assess the role of the cytoplasmic domain in intracellular trafficking of CPD, we have previously engineered the fusion protein "Alb-tail" containing the transmembrane and the cytoplasmic domains of CPD attached to the C-terminus of albumin [Varlamov et al., 2001]. When expressed in AtT-20 cells, Alb-tail demonstrated CPD-like trafficking characteristics, including localization to the TGN and slow budding from the TGN [Varlamov et al., 2001]. To examine the role of different regions of the CPD tail in intracellular routing, C-terminal deletions of Alb-tail (Fig. 1) were stably expressed in AtT-20 cells and then subjected to pulse-chase analysis. While the Δ10 mutant exhibits a half-life comparable to Alb-tail, the Δ28 and Δ38 deletions demonstrate a dramatic reduction in stability (Fig. 2A). In contrast, the Δ49 mutant shows an increased half-life (Fig. 2A).

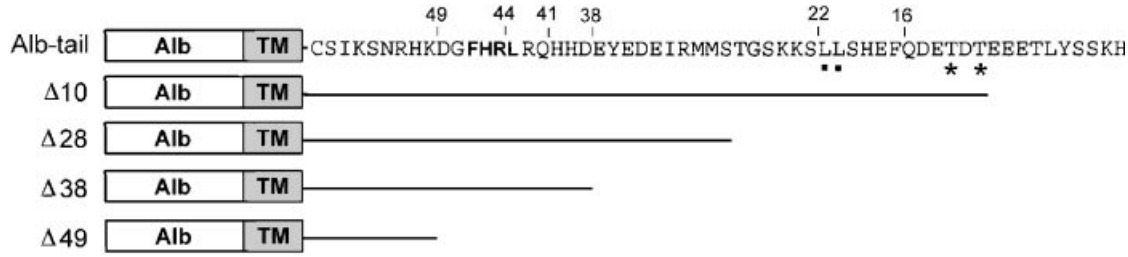

Fig. 1. Deletion mutants of the CPD tail attached to the C-terminus of albumin used in the present study. The YxxL-like sequence FHRL (in bold type), the CK2 sites (asterisks), and a di-leucine motif (squares) are indicated. Numbers correspond to the length of the deletion (from the C-terminus). The albumin (Alb) and CPD transmembrane (TM) regions are not drawn to scale.

To examine whether the increased turnover rates of the C-terminal deletion constructs are due to the loss of TGN retention, we utilized an in vitro budding assay that measures the formation of nascent secretory vesicles from the TGN [Varlamov et al., 1999b]. While Alb-tail enters vesicles with a very low efficiency (5%), the Δ10, Δ28, and Δ38 mutants show a significantly higher budding efficiency (20–30%) (Fig. 2B). In contrast, the Δ49 mutant enters vesicles with a low efficiency (Fig. 2B). The difference in budding is not due to a clonal variation; several clones expressing each construct were examined with similar results. In addition, the budding of carboxypeptidase E was approximately 30% in all cell lines shown in Figure 2, indicating little clonal variation in the various lines.

The loss of TGN retention of the deletion mutants was expected to increase the trafficking of the proteins to the cell surface. To test this, we measured the rate of cell surface biotinylation of newly synthesized proteins. While only 5% of the total labeled Alb-tail is delivered from the TGN to the cell surface by 2 h of incubation, the Δ38 mutant rapidly appears at the cell surface (Fig. 3). By 2 h of incubation, nearly 100% of the Δ38 mutant has become biotinylated (Fig. 3).

To determine whether the cytoplasmic tail modulates the endocytic uptake of Alb-tail from the cell surface, we utilized a cell surface

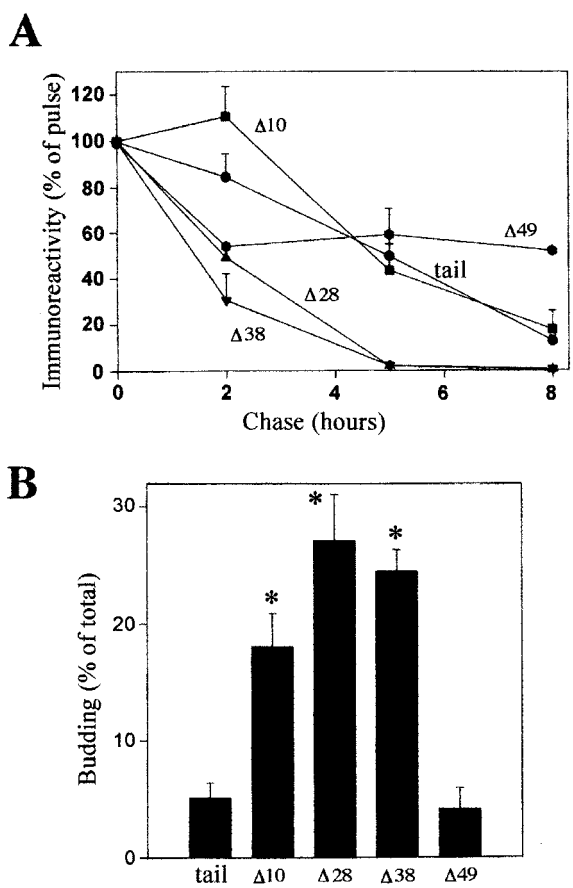

Fig. 2. Pulse-chase analysis and budding from the TGN of deletion mutants. **A**: AtT-20 cells expressing Alb-tail and deletion mutants of the CPD tail were metabolically labeled for 15 min with [^{35}S]Met (pulse), and then chased for the indicated periods of time. Proteins were isolated by immunoprecipitation and analyzed as described in Materials and Methods. Error bars indicate range of duplicate determinations. Two different cell lines were analyzed for each construct with similar results. Circles, wild-type CPD tail; squares, Δ10; triangles, Δ28; inverted triangles, Δ38; hexagons, Δ49. **B**: Packaging of deletion mutants into nascent vesicles in AtT-20 cells. To assay for nascent vesicles, AtT-20 cells were pulse-labeled with [^{35}S]Met and then chased for 2 h at 18.5°C to accumulate radiolabeled proteins in the TGN, permeabilized, and then incubated in the presence of an energy-generating system as described [Varlamov et al., 1999b]. The efficiency of budding is calculated as the ratio of radiolabeled albumin immunoreactivity in the vesicle fraction (after subtraction of the background measured in the absence of energy) relative to the total amount of radiolabeled albumin immunoreactivity. Error bars indicate standard error of the mean, n = 4. Statistical significance compared to the wild-type tail was determined using Student's *t*-test: $^*P < 0.01$.

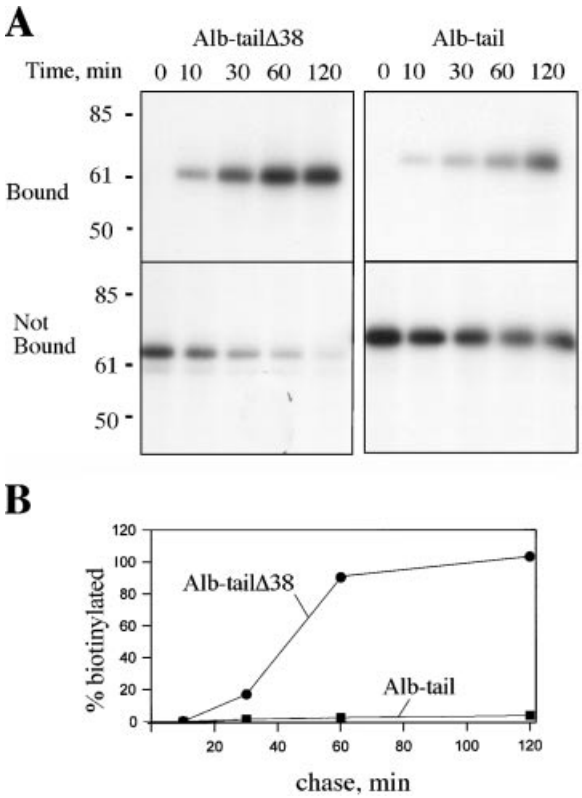

Fig. 3. Trafficking of Alb-tail and the C-terminally truncated mutant Δ38 between the TGN and the cell surface. **A**: AtT-20 cells expressing Alb-tail or Alb-tailΔ38 were pulse-labeled with [^{35}S]Met, chased for 2 h at 18.5°C to accumulate radiolabeled proteins in the TGN, and then incubated at 37°C in the presence of membrane-impermeable biotin for the indicated periods of time (in minutes). The albumin fusion proteins were isolated by immunoprecipitation, and then the biotinylated, cell surface-derived pool of the proteins was selected by streptavidin-agarose as described in Materials and Methods. The entire amount of the streptavidin-agarose-bound Alb-tail and Alb-tailΔ38 fractions, and 7% of the unbound fractions, were loaded onto a polyacrylamide gel. The positions of prestained size standards (in kDa) are indicated. **B**: Percentage of the indicated radiolabeled protein that traveled to the cell surface and became biotinylated (i.e., the bound fraction in Panel A) relative to the total radiolabeled protein (i.e., the sum of bound and unbound fractions after correction for the amount of each fraction loaded onto the gels in Panel A). The experiment was performed twice with similar results.

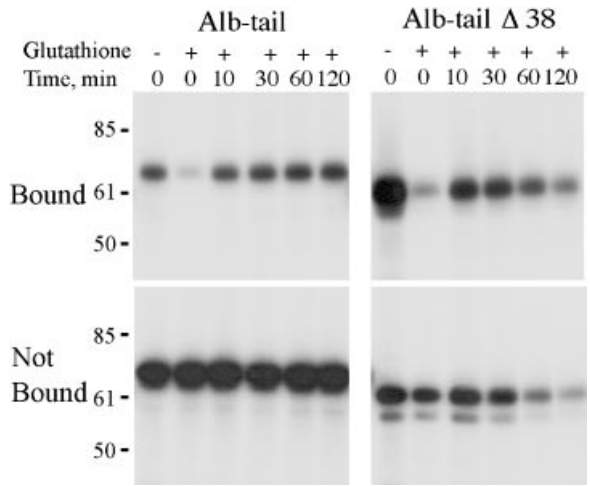

Fig. 4. Endocytosis of the Alb-tail deletion mutants from the cell surface of AtT-20 cells. [^{35}S]Met-labeled AtT-20 cells were subjected to cell surface biotinylation at 4°C, and then chased for the indicated periods of time at 37°C. The cells were treated with glutathione to remove the cell surface-associated biotin, lysed, and then processed as described above to select the biotinylated pool of Alb-tail or Alb-tailΔ38. One hundred percent of the streptavidin-agarose bound material and 5.5% of the unbound material was analyzed on a polyacrylamide gel. The positions of prestained size standards (in kDa) are indicated. The experiment was performed twice with similar results.

biotinylation technique to measure the rate of internalization of Alb-tail and the Δ38 mutant. The bulk of Alb-tail that is biotinylated on the cell surface becomes resistant to glutathione after 10 min of incubation at 37°C, indicating that this protein is rapidly internalized from the cell surface (Fig. 4, left panels). Further incubation does not result in degradation of the cell surface-derived Alb-tail (Fig. 4, left panels) indicating that the majority of the internalized Alb-tail bypassed the degradation compartment. Although the Δ38 mutant is also internalized from the cell surface, a large fraction of the protein is degraded in 1 h of incubation (Fig. 4, right panels).

Although we previously examined the uptake of full-length duck CPD and several C-terminal deletion mutants in the AtT-20 cell line [Eng et al., 1999], it was not clear if the lumenal portion of the protein contributed to the routing. Thus, it was important to determine whether similar results could be obtained when the lumenal part of CPD was replaced with Alb. AtT-20 cells expressing various deletion mutants were incubated with an antiserum to albumin and then subjected to indirect immunofluorescence. While both Alb-tail and the Δ10 mutant are delivered to a perinuclear compartment within 30 min of uptake, the Δ28 mutant demonstrates an additional punctate staining, which is more profound for the Δ38 mutant (Fig. 5A). The perinuclear compartment containing the internalized Alb-tail and various mutants (except Δ49) co-stains with antiserum directed against the TGN marker syntaxin-6 (Fig. 5B). In addition, this perinuclear compartment also contains internalized transferrin (Fig. 5B). However, the non-perinuclear punctate staining of the Δ28 and Δ38 mutants found throughout the

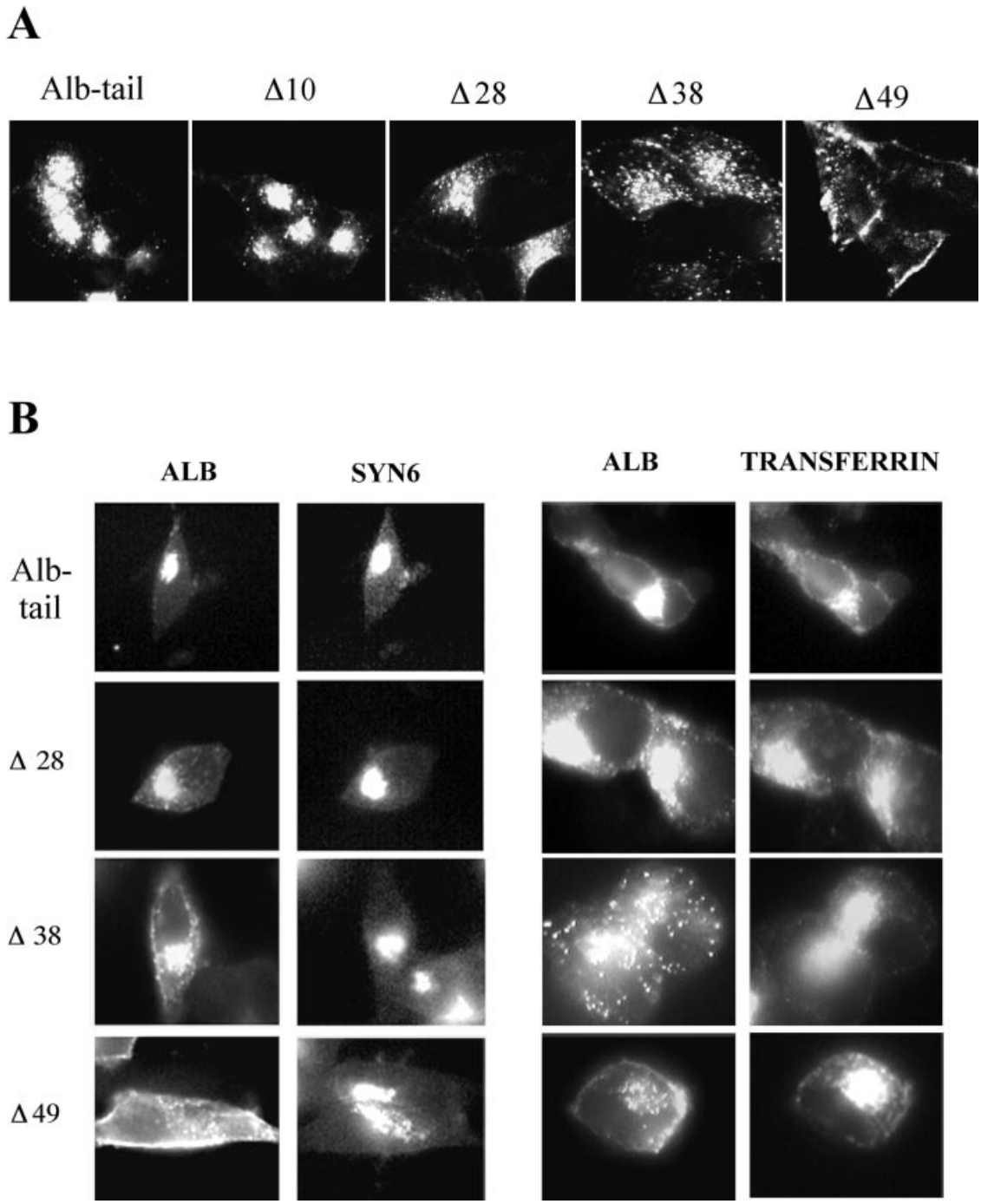

Fig. 5. Internalization of antibodies to albumin into AtT-20 cells expressing Alb-tail or the deletion mutants. **A**: Cells were preincubated on ice with antibodies to albumin for 40 min, washed, chased at 37°C for 30 min, and then subjected to indirect immunofluorescence as described in Materials and Methods. **B**: Cells were treated as described in Panel A and then were additionally stained with a mouse monoclonal antibody to syntaxin-6 (SYN-6), as described in Materials and Methods. In a separate experiment, cells were treated as described in Panel A except that CY3-labeled transferrin was added during the 30 min chase.

cytoplasm does not overlap with syntaxin-6 and only partially overlaps with transferrin (Fig. 5B). This suggests that these mutants are present in a compartment distinct from the TGN or endocytic recycling compartment. In contrast to the other mutants, the internalized Δ49 mutant is primarily localized in structures on or near the cell surface (Fig. 5A). In addition,

lower levels of internalized Δ49 mutant are seen in punctate structures throughout the cytoplasm; this punctate staining partially overlaps with internalized transferrin, but not with syntaxin-6 (Fig. 5B). These results are generally similar to those previously found with constructs containing the CPD luminal domain, instead of the Alb used in the present study, indicating that the CPD transmembrane domain and tail are sufficient for the proper routing of the protein [Eng et al., 1999].

We have previously shown that the CPD tail is primarily phosphorylated at the CK2 sites (TDT) in vitro and in vivo [Varlamov et al., 2001]. To elucidate the significance of the CK2 sites in vivo, these sites within Alb-tail were mutated either to Ala (ADA) to mimic the unphosphorylated form or to Glu (EDE) to mimic the phosphorylated form. While the half-life of the EDE mutant is similar to that of Alb-tail, the ADA mutant exhibits a significantly reduced stability after 4 h of incubation (Fig. 6A). Interestingly, mutation of the di-leucine motif to Ala also has a de-stabilizing effect on the protein (Fig. 6A). Although the ADA mutant demonstrated a reduced half-life, it enters the post-TGN vesicles with a rate that is similar to that of Alb-tail and the AA mutant (Fig. 6B). Although the EDE mutant has a slightly reduced rate of budding, this is not statistically different from the rate of the wild type tail (Fig. 6B). All of the point mutants are predominantly located in the perinuclear region of AtT-20 cells (Fig. 7). This pattern is consistent with the TGN-localization of CPD [Varlamov and Fricker, 1998]. In addition to the perinuclear staining, the ADA mutant demonstrates small accumulation in the tips of AtT-20 cells (Fig. 7). This staining of the tips is not seen for the other mutants examined (Fig. 7) or for wild-type CPD [Varlamov and Fricker, 1998], but is observed for carboxypeptidase E and other proteins routed to the regulated secretory pathway [Varlamov and Fricker, 1998].

The cytoplasmic tail of CPD contains several motifs including the YxxL-like FHRL sequence and the CK2 sites that regulate the trafficking of several other proteins within the TGN-endosomal system through the binding of different sets of adaptor proteins [Rohn et al., 2000]. To test the ability of the C-terminal deletion mutants to bind adaptors either directly or indirectly (i.e., through other proteins), we incubated the GST-CPD tail fusion

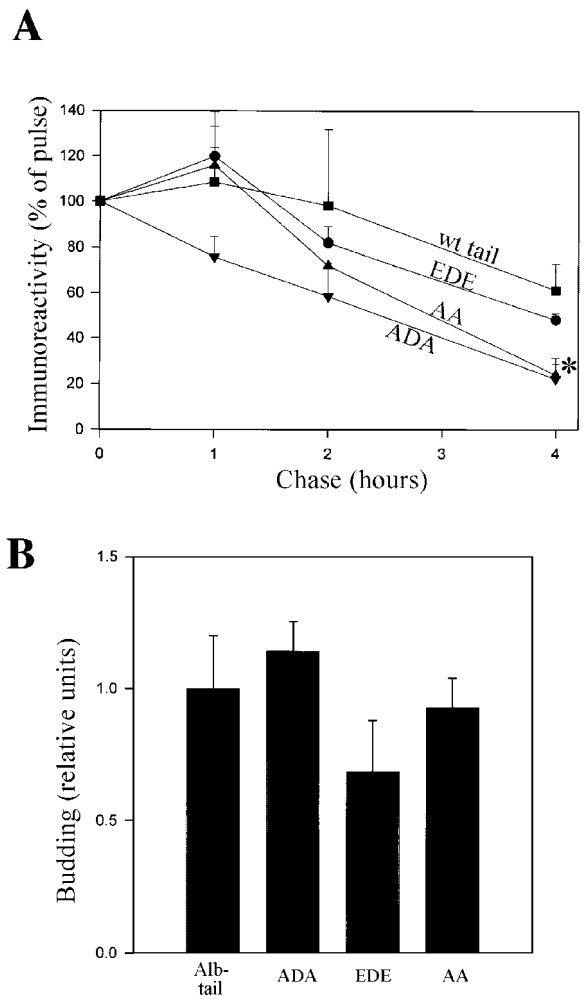

Fig. 6. Pulse-chase analysis and budding from the TGN of point mutants. **A**: AtT-20 cells expressing the Alb-tail point mutants were subjected to [^{35}S]Met pulse-chase analysis as described in Materials and Methods and in legend of Figure 2. Error bars indicate standard error of the mean, n = 4. Statistical significance was determined using Student's *t*-test: $^{*}P < 0.01$ compared to wild-type CPD tail. Squares, wild-type CPD tail; circles, TDT to EDE; triangles, LL to AA; inverted triangles, TDT to ADA. **B**: Packaging of point mutants into nascent vesicles in AtT-20 cells was performed as described in Materials and Methods and legend of Figure 2. Graph shows the efficiency of budding of the mutants as compared with Alb-tail. Error bars indicate range of duplicate determinations. The experiment was performed twice with similar results.

proteins with bovine brain cytosol, and then analyzed the GST-CPD tail-bound material on a Western blot using antibodies to AP-1 and AP-2. While the full-length CPD tail is not able to bind AP-1 to a greater extent than the GST control (Fig. 8A), nearly all of the deletion mutants bind AP-1 (Fig. 8A, Δ10–Δ44). The Δ49 mutant that lacks the FHRL sequence does not bind AP-1 (Fig. 8A). Similarly, a point mutant in the Δ39

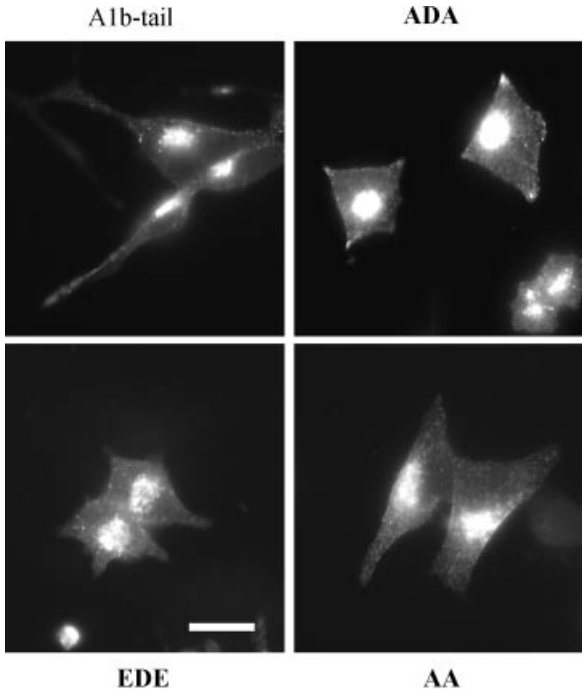

Fig. 7. Immunocytochemistry of AtT-20 cells expressing Alb-tail and point mutants (''ADA,'' TDT to ADA; ''EDE,'' TDT to EDE; ''AA,'' LL to AA). Cells were fixed and then stained with antibodies to albumin as described in Materials and Methods. Bar: 20 μm.

construct in which the Phe residue within the FHRL sequence was replaced with an Ala residue (Δ39F/A) is also unable to bind AP-1 (Fig. 8A). The construct with the CK2 site (TDT) mutated to EDE shows greatly elevated binding of AP-1, whereas mutation of this site to ADA was not significantly different from the GST control (Fig. 8A). The binding of AP-2 to the CPD tail demonstrates a generally similar tendency; while neither the full-length tail nor the mutants of the FHRL sequence significantly bind AP-2, many of the other constructs bind AP-2 (Fig. 8B). Although the intermediate deletions (Δ18–Δ28) show a slight increase in AP-2 binding over the GST control, this difference is not significant. The decrease in binding between the Δ16 and the Δ18 constructs, and the increase again between Δ28 and Δ38 mutants may be due to structural changes. As found for

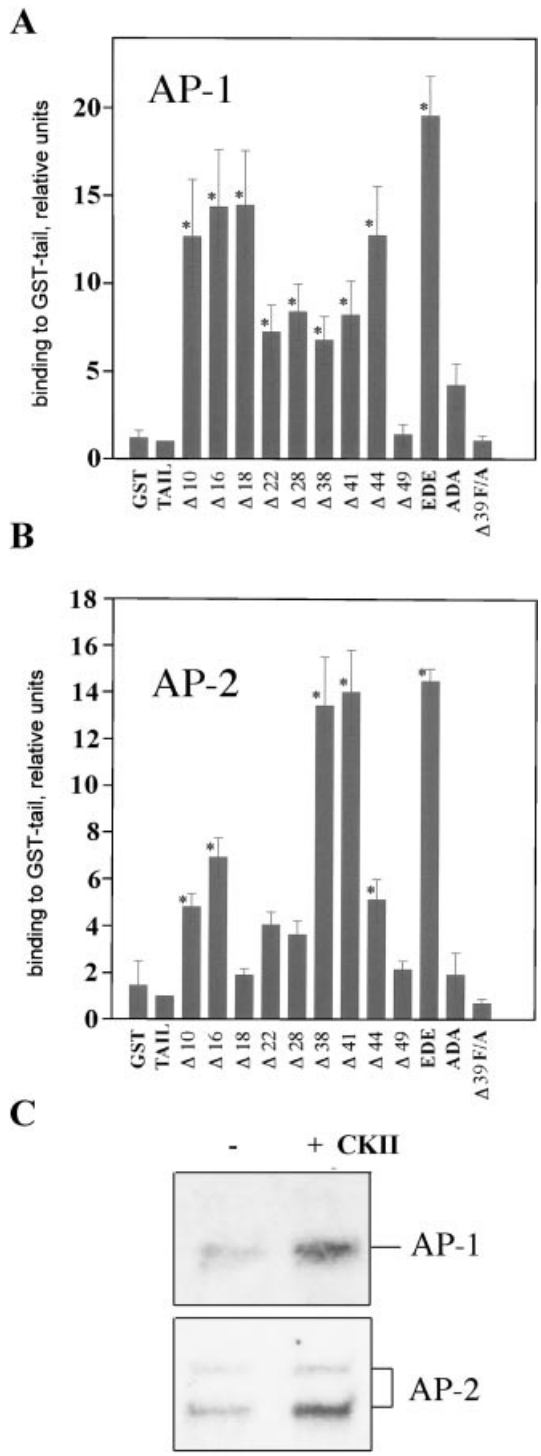

Fig. 8. Binding of adaptor proteins to the deletions of the CPD tail in vitro. **A**, **B**: Deletions of the CPD tail fused with GST were incubated for 40 min at 37°C with bovine brain cytosol, and then with glutathione-agarose for an additional 30 min. The beads containing GST fusion proteins were washed, boiled in SDS-loading buffer, and then analyzed on a Western blot using antibodies to AP-1 (Panel A) and AP-2 (Panel B). Error bars show standard error of the mean for triplicate determinations. *Statistically different from the GST control ($P < 0.05$) using Student's *t*-test. **C**: Effect of CK2 phosphorylation on the binding of AP-1 and AP-2. The full-length CPD tail attached to GST was phosphorylated with CK2, immobilized to the glutathione-agarose beads, washed, and incubated with bovine brain cytosol in the presence of phosphatase inhibitors. Bound proteins were analyzed by Western blot analysis with antisera to the indicated proteins.

AP-1 binding, the mutation of TDT to EDE has a stimulatory effect on AP-2 binding (Fig. 8B).

The present finding that the EDE mutant binds to the adaptor proteins implicates CK2 as a possible regulator of these interactions. To test this possibility, the full-length CPD tail was first phosphorylated by CK2 in vitro and then subjected to adaptor binding in the presence of phosphatase inhibitors. Phosphorylation of the CPD tail substantially enhances the binding of both AP-1 and AP-2 indicating that CK2 may regulate adaptor binding to the CPD tail in vivo (Fig. 8C).

DISCUSSION

The purpose of the present study was to map the functional subregions of the CPD tail that are responsible for the discrete trafficking step. A major finding of the present study is that the CPD tail contains both stimulatory and inhibitory signals for TGN localization. The region of the tail containing the FHRL sequence is likely to be a positive signal both for the export of CPD from the TGN (Fig. 2B, compare Δ38 and Δ49) and for endocytosis (Fig. 5). Since this sequence is crucial for the binding of both AP-1 and AP-2 in vitro, it is likely that these adaptor proteins regulate the recruitment of the CPD tail into clathrin-coated vesicles in the TGN and at the plasma membrane.

The region of the tail distal to the FHRL sequence seems to function as a negative regulator of exit from the TGN; deletions of the extreme C-terminal region greatly increase TGN export. One possible interpretation of these results is that the C-terminus of the CPD tail binds to a TGN-resident protein, thus slowing CPD entry into nascent secretory vesicles. In addition, this C-terminal domain may function as a conformational switch that regulates the access of adaptor proteins to FHRL and/or other sequences. This model is supported by the finding that removal of C-terminal sequences substantially enhances binding of the adaptors to the cytoplasmic tail. Although cleavage of the tail is not likely to occur in vivo, it is possible that phosphorylation at the CK2 sites produces a conformational change; this phosphorylation presumably occurs in vivo [Varlamov et al., 2001]. Consistent with this model is our finding that both the CK2-phosphorylated CPD tail and the EDE mutant bind AP-1 and AP-2 either directly or indirectly, whereas the unphosphorylated CPD tail does not show any binding above background. However, the finding that the Δ10 construct enters nascent vesicles much more efficiently than the ADA or EDE mutants implies that the deletion construct is missing more than just the CK2 consensus site, and that there is a static TGN retention signal that is independent of the CK2 sites.

It is possible that phosphorylation at the CK2 site facilitates the CPD retrieval step in post-TGN endosomes or immature vesicles by allowing the CPD tail to bind AP-1. A similar model has been proposed in which furin is efficiently retrieved from post-TGN compartments by the PACS-1/AP-1 mechanism [Wan et al., 1998; Molloy et al., 1999]. The mutations of the CK2 sites in the cytoplasmic tails of CPD (Fig. 7, ADA) and furin results in missorting of these proteins to the tips of AtT-20 cells, which resemble the mature secretory granules [Dittie et al., 1997]. Although AP-1 binds the phosphorylated form of the CPD tail either directly or indirectly, it is not clear whether the same adaptor regulates the TGN export and retrieval of CPD. Recently discovered AP-3 and AP-4 may provide additional machinery that regulates protein sorting in the TGN [Rohn et al., 2000].

The data presented in this article together with our previous results [Varlamov and Fricker, 1998; Eng et al., 1999; Varlamov et al., 1999a] indicate that CPD requires both static retention and retrieval for efficient localization to the TGN. This finding resembles earlier work on the cytoplasmic tail of the yeast dipeptidyl aminopeptidase A that contains both a static retention signal that keeps the protein in the TGN and a FXFXD motif, which directs retrieval to the TGN from the prevacuolar compartment [Bryant and Stevens, 1997]. A similar aromatic residue-containing signal has been identified in the cytoplasmic tail of Kex2p [Wilcox et al., 1992]. While the components of the retrieval machinery in yeast have been identified [Brickner and Fuller, 1997; Bryant et al., 1998; Voos and Stevens, 1998; Conibear and Stevens, 2000], the mechanism of static TGN retention in mammalian cells remains unknown. The loss of TGN retention of the CPD deletion mutants correlates with the increased degradation rate and appearance of the proteins at the cell surface, presumably due to a greater flux in the post-TGN pathway. Another possibility is that the deletion of the C-terminal segments of CPD results in missorting of the mutant proteins from the post-TGN retrieval

endosomes to lysosomes and to the cell surface. Although deletion of the C-terminal 38 residues of the CPD tail dramatically increases the rate of trafficking to the cell surface (Fig. 3), the endocytic uptake of this truncation mutant is also affected resulting in the missorting of internalized protein (Fig. 5). Interestingly, both the EDE mutant and the CK2-phosphorylated tail show an enhanced binding of AP-2, raising the possibility that phosphorylation at the CK2 site regulates AP-2 binding and the cycling of CPD between endosomes and the cell surface. This is consistent with an earlier report that CK2 regulates the cycling of furin between endosomes and the cell surface [Molloy et al., 1998].

In conclusion, we have identified several functional subregions within the CPD tail (Fig. 9). The FHRL sequence, which binds AP-1 and AP-2, functions as a positive signal both for TGN export/retrieval and endocytosis from the plasma membrane. In addition to the FxxL motif, the di-Leu sequence may also participate in AP-1 binding based on the deletion analysis (Fig. 8A) and the decreased half-life of the LL to AA mutant (Fig. 6A). This model is consistent with other studies, which have shown that AP-1 binds to di-Leu and is involved in the retrieval of proteins from the endosomes to the TGN [Rapoport et al., 1998]. Binding of AP-1 and AP-2 to CPD requires phosphorylation at the CK2 site (Fig. 8C), possibly due to a structural change induced by this phosphorylation. However, this phosphorylation alone is not sufficient to release CPD from a hypothetical TGN protein that binds to the acidic cluster, within the C-terminal 10 amino acids of CPD, and slows the rate of entry into nascent vesicles. The release of CPD from this hypothetical binding protein may either be catalyzed by some unknown event or it may be a spontaneous event such that the bound and unbound forms are in equilibrium. It is likely that phosphorylated CPD is recognized by PACS1 in addition to AP-1 and AP-2, and that PACS1 binding facilitates the return of phosphorylated CPD to the TGN. It is not clear if CPD is dephosphorylated during this cycle; we have previously found that protein phosphatase 2A binds to the cytosolic tail of CPD as well as other TGN proteins and is able to dephosphorylate CPD [Varlamov et al., 2001]. The events at the cell surface, although not as well defined in the present study as the TGN trafficking events, appear to involve at least the binding of AP-2 to the FxxL motif (Fig. 9). As with the binding of AP-1, the binding of AP-2 requires prior phosphorylation at the CK2 site. Further studies are needed to identify the intracellular location of the phosphorylation and dephosphorylation steps as well as the hypothetical protein that binds to the CPD tail in the TGN.

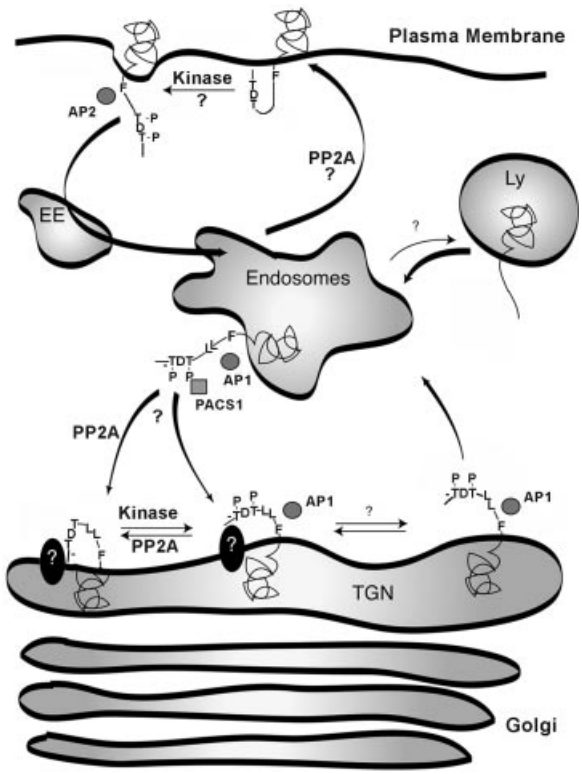

Fig. 9. Model of the trafficking of CPD and the role of specific regions within the cytosolic tail. Residues indicated within the CPD cytosolic tail include the Phe of the FHRL sequence (F), the di-Leu sequence (LL), the CK2-like phosphorylation site (TDT), and the acidic cluster within the C-terminal 10 amino acids (—). Ly, lysosomes; EE, early endosomes; PP2A, protein phosphatase 2A.

ACKNOWLEDGMENTS

The DNA sequencing facility of the Albert Einstein College of Medicine is supported in part by Cancer Center grant CA13330. Fluorescent microscopy was performed in the Laboratory of Dr. Jonathan Backer at the Department of Molecular Pharmacology of the Albert Einstein College of Medicine. Thanks to Gary Thomas for helpful discussions.

REFERENCES

Brickner JH, Fuller RS. 1997. SOI1 encodes a novel, conserved protein that promotes TGN-endosomal cycling of Kex2p and other membrane proteins by modulating

the function of two TGN localization signals. J Cell Biol 139:23–36.

Bryant NJ, Stevens TH. 1997. Two separate signals act independently to localize a yeast late Golgi membrane protein through a combination if retrieval and retention. J Cell Biol 136:287–297.

Bryant NJ, Piper RC, Weisman LS, Stevens TH. 1998. Retrograde traffic out of the yeast vacuole to the TGN occurs via the prevacuolar/endosomal compartment. J Cell Biol 142:651–663.

Cain BM, Wang W, Beinfeld MC. 1997. Cholecystokinin (CCK) levels are greatly reduced in the brains but not the duodenums of Cpe^{fat}/Cpe^{fat} mice: a regional difference in the involvement of carboxypeptidase E (Cpe) in pro-CCK processing. Endocrinol 138:4034–4037.

Conibear E, Stevens TH. 2000. Vps52p, Vps53p, and Vps54p from a novel multisubunit complex required for protein sorting at the yeast late Golgi. Mol Biol Cell 11:305–323.

Dittie AS, Thomas L, Thomas G, Tooze SA. 1997. Interaction of furin in immature secretory granules from neuroendocrine cells with the AP-1 adaptor complex is modulated by casein kinase II phosphorylation. EMBO J 16:4859–4870.

Eng FJ, Varlamov O, Fricker LD. 1999. Sequences within the cytoplasmic domain of gp180/carboxypeptidase D mediate localization to the *trans*-Golgi network. Mol Biol Cell 10:35–46.

Fricker LD. 1998a. Carboxypeptidase E/H. In: Barrett AJ, Rawlings ND, Woessner JF, editors. Handbook of proteolytic enzymes. San Diego: Academic Press. p 1341–1344.

Fricker LD. 1998b. Metallocarboxypeptidase D. In: Barrett AJ, Rawlings ND, Woessner JF, editors. Handbook of proteolytic enzymes. San Diego: Academic Press. p 1349–1351.

Fricker LD, Das B, Angeletti RH. 1990. Identification of the pH-dependent membrane anchor of carboxypeptidase E (EC 3.4.17.10). J Biol Chem 265:2476–2482.

Fricker LD, Berman YL, Leiter EH, Devi LA. 1996. Carboxypeptidase E activity is deficient in mice with the *fat* mutation: effect on peptide processing. J Biol Chem 271:30619–30624.

Kuroki K, Eng F, Ishikawa T, Turck C, Harada F, Ganem D. 1995. gp180, a host cell glycoprotein that binds duck hepatitis B virus particles, is encoded by a member of the carboxypeptidase gene family. J Biol Chem 270:15022–15028.

Lacourse KA, Friis-Hansen L, Rehfeld JF, Samuelson LC. 1997. Disturbed progastrin processing in carboxypeptidase E-deficient *fat* mice. FEBS Lett 416:45–50.

Milgram SL, Mains RE. 1994. Differential effects of temperature blockade on the proteolytic processing of three secretory granule-associated proteins. J Cell Sci 107:737–745.

Molloy SS, Thomas L, Kamibayashi C, Mumby MC, Thomas G. 1998. Regulation of endosome sorting by a specific PP2A isoform. J Cell Biol 142:1399–1411.

Molloy SS, Anderson ED, Jean F, Thomas G. 1999. Bicycling the furin pathway: from TGN localization to pathogen activation and embryogenesis. Trends Cell Biol 9:28–35.

Naggert JK, Fricker LD, Varlamov O, Nishina PM, Rouille Y, Steiner DF, Carroll RJ, Paigen BJ, Leiter EH. 1995. Hyperproinsulinemia in obese *fat*/*fat* mice associated with a point mutation in the carboxypeptidase E gene and reduced carboxypeptidase E activity in the pancreatic islets. Nat Genet 10:135–142.

Rapoport I, Chen YC, Cupers P, Shoelson SE, Kirchhausen T. 1998. Dileucine-based sorting signals bind to the β chain of AP-1 at a site distinct and regulated differently from the tyrosine-based motif-binding site. EMBO J 17:2148–2155.

Rohn WM, Rouille Y, Waguri S, Hoflack B. 2000. Bidirectional trafficking between the trans-Golgi network and the endosomal/lysosomal system. J Cell Sci 113: 2093–2101.

Rovere C, Viale A, Nahon J, Kitabgi P. 1996. Impaired processing of brain proneurotensin and promelanin-concentrating hormone in obese *fat*/*fat* mice. Endocrinol 137:2954–2958.

Song L, Fricker LD. 1995. Purification and characterization of carboxypeptidase D, a novel carboxypeptidase E-like enzyme, from bovine pituitary. J Biol Chem 270:25007–25013.

Song L, Fricker LD. 1996. Tissue distribution and characterization of soluble and membrane-bound forms of metallocarboxypeptidase D. J Biol Chem 271:28884–28889.

Tan F, Rehli M, Krause SW, Skidgel RA. 1997. Sequence of human carboxypeptidase D reveals it to be a member of the regulatory carboxypeptidase family with three tandem active site domains. Biochem J 327:81–87.

Udupi V, Gomez P, Song L, Varlamov O, Reed JT, Leiter EH, Fricker LD, Greeley GHJ. 1997. Effect of carboxypeptidase E deficiency on progastrin processing and gastrin mRNA expression in mice with the *fat* mutation. Endocrinol 138:1959–1963.

Varlamov O, Fricker LD. 1998. Intracellular trafficking of metallocarboxypeptidase D in AtT-20 cells: localization to the *trans*-Golgi network and recycling from the cell surface. J Cell Sci 111:877–885.

Varlamov O, Eng FJ, Novikova EG, Fricker LD. 1999a. Localization of metallocarboxypeptidase D in AtT-20 cells: potential role in prohormone processing. J Biol Chem 274:14759–14767.

Varlamov O, Wu F, Shields D, Fricker LD. 1999b. Biosynthesis and packaging of carboxypeptidase D into nascent secretory vesicles in pituitary cell lines. J Biol Chem 274:14040–14045.

Varlamov O, Kalinina E, Che F, Fricker LD. 2001. Protein phosphatase 2A binds to the cytoplasmic tail of carboxypeptidase D and regulates post-TGN trafficking. J Cell Sci 114:311–322.

Voos W, Stevens TH. 1998. Retrieval of resident late-golgi membrane proteins from the prevacuolar compartment of *Saccharomyces cerevisiae* is dependent on the function of Grd19p. J Cell Biol 140:577–590.

Wan L, Molloy SS, Thomas L, Liu G, Xiang Y, Rybak SL, Thomas G. 1998. PACS-1 defines a novel gene family of cytosolic sorting proteins required for *trans*-Golgi network localization. Cell 94:205–216.

Wilcox CA, Redding K, Wright R, Fuller RS. 1992. Mutation of a tyrosine localization signal in the cytosolic tail of yeast Kex2 protease disrupts Golgi retention and results in default transport to vacuole. Mol Biol Cell 3:1353–1371.

Xin X, Varlamov O, Day R, Dong W, Bridgett MM, Leiter EH, Fricker LD. 1997. Cloning and sequence analysis of cDNA encoding rat carboxypeptidase D. DNA Cell Biol 16:897–909.